ASTRONOMY & ASTROPHYSICS
SUPPLEMENT SERIES

Astron. Astrophys. Suppl. Ser. **137**, 473–493 (1999)

Spectral classification of the cool giants in symbiotic systems⋆

U. Mürset[1] **and H.M. Schmid**[2]

[1] Institut für Astronomie, ETH Zentrum, CH-8092 Zürich, Switzerland
e-mail: muerset@astro.phys.ethz.ch
[2] Landessternwarte Heidelberg-Königstuhl, D-69117 Heidelberg, Germany
e-mail: hschmid@lsw.uni-heidelberg.de

Received December 21, 1998; accepted March 23, 1999

Abstract. We derive the spectral types of the cool giants in about 100 symbiotic systems. Our classification is mainly based on near IR spectra in order to avoid the contamination of the spectrum by the nebula and the hot component in the visual region. The accuracy of our spectral types is approximately one spectral subclass, similar to previous near IR classification work, and much better than visual spectral type estimates.

Strong, intrinsic spectral type variations (> 2 spectral subtypes) are only seen in systems containing pulsating mira variables.

We present a catalogue of spectral types for cool giants in symbiotic systems which also includes determinations taken from the literature. The catalogue gives spectral types for the cool giants in about 170 systems which is nearly the full set of confirmed symbiotics.

Based on our classifications we discuss the distribution of spectral types of the cool giants in galactic symbiotic binaries. We find that the spectral types cluster strongly between M3 and M6, with a peak at M5. The distribution of systems with a mira variable component peaks even later, at spectral types M6 and M7. This is a strong bias towards late spectral types when compared to red giants in the solar neighbourhood. Also the frequency of mira variables is much larger among symbiotic giants. This predominance of very late M-giants in symbiotic systems seems to indicate that large mass loss is a key ingredient for triggering symbiotic activity on a white dwarf companion.

Further we find for symbiotic systems a strong correlation between the spectral type of the cool giant and the orbital period. In particular we find a tight relation for the minimum orbital period for symbiotic systems with red giants of a given spectral type. This limiting line in the spectral type – orbital period diagram seems to be equivalent with the relation $R \leq \ell_1/2$, where R is the radius of the red giant and ℓ_1 the distance from the center of the giant to the inner Lagrangian point L_1. This correlation possibly discloses that symbiotic stars are – with probably only one exception in our sample – well detached binary systems.

Key words: binaries: symbiotic — stars: fundamental parameters — stars: late-type — stars: mass-loss — novae, cataclysmic variables

1. Introduction

Symbiotic stars are closely related to the cataclysmic variables, in the sense that a white dwarf's activity is triggered by mass transfer from a cool companion star. But the cool star in symbiotic systems is a giant rather than a dwarf as in the case of cataclysmic systems. The orbits of symbiotic systems are correspondingly wide ($P > 200$ d). The nature of the interactions and of the activity of the white dwarf are still a matter of debate. In any case the fundamental characteristics of the red giant donor are certainly an important factor. The spectral type of red giant branch or asymptotic giant branch stars is strongly correlated with stellar radius and probably also with mass loss. Both, radius and mass loss are important parameters in interacting binaries. Thus, a significant sample of accurate spectral classifications may clarify some aspects of the interaction processes in symbiotic stars.

Spectral classifications of cool giants of symbiotic systems are widely scattered in the literature. A compilation of early classifications is given in Allen (1982). However, these spectral types are based on various classification criteria and their quality is often rather crude. Sophisticated

⋆ Based on observations obtained with the 1.52 m and 3.6 m telescopes of the European Southern Observatory (ESO), the 1.93 m telescope of the Observatoire de Haute-Provence (OHP), the 2.3 m telescope of the Australian National University (ANU) at Siding Spring, and the William Herschel Telescope (WHT) at La Palma. This research has made use of the AFOEV database, operated at CDS, France.

and devoted classification work has been published by Kenyon & Fernández-Castro (1987) and Schulte-Ladbeck (1988). These papers are, however, restricted to about three dozen bright objects. Recent classifications can be found in the extended lists of Medina Tanco & Steiner (1995), Harries & Howarth (1996), and Mikołajewska et al. (1997). These studies employed, however, spectra with restricted resolution or spectral coverage which may cause some larger uncertainties in the resulting spectral types.

Determining the spectral types of cool giants in symbiotic systems is complicated by the composite nature of the spectra. Often the blue spectral region, according to which the classification of "normal" stars is traditionally done, is strongly contaminated by light from the circumstellar nebula and/or from the hot companion. Therefore, the spectral classification of cool giants in symbiotic systems should be done in the near IR region, which offers a number of decisive advantages:

- In the near IR the cool star is usually the dominant spectral component while the contributions from the nebula and from the hot star decrease towards longer wavelengths.
- The near IR is full of telltale molecular bands formed in the atmosphere of the cool giant. These bands are temperature sensitive and well suited for spectral classification.
- In the near IR the red giants are bright enough to be observed with relatively short exposure times.

After describing the spectroscopic data in Sect. 2, we derive in Sect. 3 the spectral types for the cool giants in about 100 symbiotic systems. We compare our results with previous studies and discuss the accuracy of our classification. Supplementary spectral types are taken from the literature and are included in a catalogue (Sect. 4, Table 5) which contains spectral types for the cool giants in about 170 systems (about 95% of all known symbiotic systems). In Sects. 5 and 6 we discuss properties of the distribution of the spectral types of the cool giants in symbiotic binaries and correlations between the spectral types and other system parameters. Considerations on the evolution of symbiotic binaries are presented in Sect. 7. Section 8 summarizes our results and conclusions.

2. Observations

Most of our data are low resolution near IR spectra of symbiotic stars. For the purpose of spectral classification, they have been complemented by a set of comparison standard star spectra. Supplementary spectra in the blue wavelength region are employed for the spectral classification of about ten symbiotic systems, which have cool giants without strong molecular bands in the near IR. The data were collected in the course of several observing runs with various instruments. The following subsections describe these instruments and the spectra obtained. A combined log of our data is given in Table 1.

2.1. ESO 1.5 m

The largest dataset (targets and spectral standard stars) was acquired in 1992 with the 1.52 m telescope of the European Southern Observatory (ESO) in La Silla, Chile. The telescope was equipped with the Boller & Chivens spectrograph and a 2k Ford Aerospace CCD (ESO #24). With grating #19 a wavelength coverage of approximately $6900 - 10\,700$ Å was achieved with a resolution of $\Delta\lambda \approx 4$ Å. An OG570 filter isolated the first spectral order.

With the same telescope, R.E. Schulte-Ladbeck had observed some systems already in 1987. She kindly made these data available to us.

2.2. OHP 1.93 m

Medium resolution spectra of northern symbiotic systems were taken at the Observatoire de Haute-Provence (OHP) in France. The spectra were obtained during six observing runs in 1988 January, June, August and December, and in 1989 May and August. We used the CARELEC spectrograph attached to the Cassegrain focus of the 1.93 m telescope. A grating with a dispersion of 33 Å/mm and a RCA CCD were used, giving a resolution of 1 Å/pixel or a FWHM of ≈ 1.8 Å for the lines of a neon calibration lamp. The observed spectral range was 8400 Å – 8900 Å except for the first run where the range was 8200 Å – 8700 Å.

Additional observations were made in August 1989 with the same equipment, but with a lower resolution grating (dispersion of 260 Å/mm). This provided spectra with a resolution of about 8 Å/pixel or a FWHM of ≈ 15 Å and a spectral coverage of 7000 Å – 11000 Å.

During the night of August 19, 1989 we have also taken spectra in the blue wavelength region with the 130 Å/mm grating. These data cover the wavelength range 3550 Å – 5550 Å with a resolution of about 7 Å (FWHM) or 4 Å/pixel. These spectra are useful for the classification of symbiotic systems with G- or K-type giants, namely AG Dra, S190, V741 Per and He2–467.

2.3. ESO 3.6 m and 4.2 m WHT

Schmid & Schild (1994) published a spectropolarimetric survey of symbiotic stars. Their Stokes I spectra are suited for our analysis as well. A detailed description of the observations can be found in their paper.

2.4. ANU 2.3 m

Additional spectra of southern symbiotic systems were collected during the nights of April 29 and 30, 1994 with the

Table 1. Spectra used in the spectral type analysis

Targets	Dates (JD)	Telescope & Instrument	Wavelength range [Å]	$\Delta\lambda$ [Å]	Note
RW Hya, Hen1103, He2–173, Hen1341, Hen1342, M1–21, Pt–1, RT Ser, AE Ara, SS96, RS Oph, AS255, AS270, AS289, AR Pav, MWC960, V919 Sgr, Hen1761	46 952/3	ESO 1.52 m, Boller & Chivens	5700 − 8100	6	1
EG And, AX Per, BX Mon, Z And, R Aqr	47 161	OHP 1.93 m, Carelec, RCA CCD	8200 − 8700	2	
EG And, AX Per, V741 Per, T CrB, AG Dra, RS Oph, AS289, YY Her, AS296, V443 Her, AS338, BF Cyg, CH Cyg, HM Sge, AS360, CI Cyg, V1016 Cyg, HBV475, S190, AG Peg, Z And	47 341, 47 377, 47 507/8, 47 664, 47 667, 47 756	OHP 1.93 m, Carelec, RCA CCD	8400 − 8900	2	
AX Per, S32, V741 Per, AG Dra, YY Her, V443 Her, AS338, BF Cyg, HM Sge, AS360, CI Cyg, PU Vul, HBV475, S190, AG Peg, Z And	47 754	OHP 1.93 m, Carelec, RCA CCD	7100 − 11 000	15	
V741 Per, AG Dra, He2–467, S190	47 758	OHP 1.93 m, Carelec, RCA CCD	3550 − 5550	7	
S32, BX Mon, MWC560, Wray157, RX Pup, Hen160, AS201, He2–38, Hen461, SS29, Hen653, SY Mus, He2–87, Hen828, SS38, Hen863, St2–22, CD–36.8436, Hen905, RW Hya, V704 Cen, He2–104, He2–106, BD–21.3873, He2–127, Hen1092, Hen1103, HD 330 036, He2–139, W16–202, He2–147, Wray1470, He2–171, Hen1213, He2–173, He2–176, Hen1242, AS210, HK Sco, CL Sco, V455 Sco, Hen1342, AS221, Hen1410, SSM1, H1–36, AS255, V2416 Sgr, H2–38, SS129, V615 Sgr, Hen1591, AS276, V2506 Sgr, SS141, Y CrA, V2756 Sgr, He2–374, AR Pav, V3811 Sgr, AS316, AS327, FN Sgr, V919 Sgr, Ap3–1, Hen1761, RR Tel, CD–43.14304 + spectral standards (cf. Table 2)	48 693 −48 698	ESO 1.52 m, Boller & Chivens, FA CCD	6900 − 10 700	4	
He2–38, SY Mus, He2–106, He2–127, Hen1242, RT Ser, AS316, AS327, RR Tel, CD–43.14304	48 802 −48 805	ESO 3.6 m, EFOSC1, TEK CCD	6700 − 8350	7	2
AG Dra, RT Ser, CI Cyg, V1016 Cyg, HBV 475, Z And	48 486 −48 488	WHT 4.2 m, ISIS, EEV CCD	6700 − 7600 (RT Ser: 6400 − 7300)	1.5	2
MWC560, Wray157, RX Pup, Hen160, AS201, He2–38, SS29, SY Mus, Hen905, RW Hya, Hen916, He2–104, He2–106, BD–21.3873, He2–127, Hen1092, HD 330 036, He2–171, He2–176, Hen1242, HK Sco, V455 Sco, Hen1341, Hen1342, H2–5, M1–21, RT Ser, H1–36, V2416 Sgr, H2–38, AR Pav, AS316, NSV11776, HM Sge, RR Tel, PU Vul, CD–43.14304, S190	49 472/3	ANU 2.3 m, DBS, Loral CCDs	6300 − 10 300 and 3300 − 5300	8 6	

Notes: 1: spectra kindly provided by R.E. Schulte-Ladbeck; 2: published by Schmid & Schild (1994).

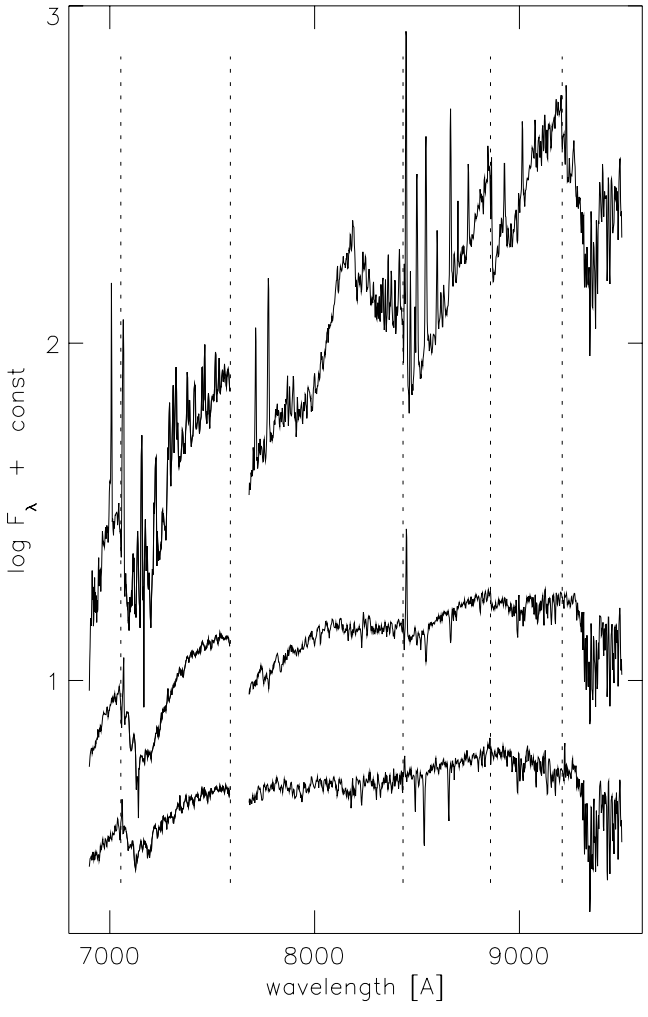

Fig. 1. Typical near IR spectra of s-type symbiotic systems containing an M-giant. The uppermost curve shows the spectrum of a system with a late M-giant (AS221, M7.5); the middle displays the M3.5 spectrum of HK Sco; the bottom spectrum is an early M–type (Hen1342, M0). The indicated TiO band heads (dotted lines) are used in the analysis. For clarity we left a gap at the location of the strongest absorptions from the telluric A band (λ7593) in order to illustrate the spectral characteristics of the TiO λ7589 band

Australian National University (ANU) 2.3 m Telescope operated by the Mount Stromlo and Siding Spring Observatory (MSSSO). We used the Double Beam Spectrograph (DBS), which splits the incoming light into a blue and a red arm with separate CCD detectors.

For the red arm a grating with 158 lines/mm provided a resolution of about 4 Å/pixel or a FWHM of $\approx$ 8 Å for the lines of a HeAr calibration lamp. The wavelength range covered was 6300 Å – 10 300 Å.

The blue arm of the DBS recorded simultaneously with the near infrared data a spectrum from 3300 Å to 5300 Å with a resolution of about 6 Å (FWHM) using a grating with 300 lines/mm. For our study we selected only the blue spectra of systems with a G or K type giant, where a spectral classification in the near infrared based on TiO bands was impossible. This sample consists of AS201, Wray157, S190, HD 330 036, BD–21.3873, and CD–43.14304.

3. Spectral classification

3.1. TiO bands in M-type and late K-type giants

M-type and late K-type stars show prominent TiO bands in the near IR (cf. Fig. 1). It is well established that the strengths of these bands correlate tightly with spectral type (e.g. Keenan & Hynek 1945; Sharpless 1956; Ramsey 1981; Kenyon & Fernández-Castro 1987; Schild et al. 1992). Kenyon & Fernández-Castro (1987) and Schulte-Ladbeck (1988) succesfully classified symbiotic spectra using these bands. We basically apply their methods to a larger sample of targets. For our classification we use the depths of the heads of the strong TiO bands at $\lambda\lambda$7054, 7589, 8432, 8859, and 9209.

We determined the spectral types by comparing the strengths of the TiO band heads of the target stars to those of the spectral standards. We either carried out the comparison "by eye", or we judged the ratio of the two spectra. Figure 2 shows an example. In this procedure we payed particular attention to the different spectral resolution and spectral coverage of our spectra. Especially the spectral types derived from the low resolution ($\Delta\lambda$ = 15 Å) spectra taken during the run at OHP on JD 47754 should be considered with caution, as numerous weak emission lines may veil the molecular absorptions. Fortunately, the majority of these observations can be checked with higher resolution spectra, which were taken two days later.

The standard stars we used are listed in Table 2. We selected them from the catalogue of Keenan & McNeil (1989). A classification system restricted to "half" subtypes (i.e. M0, M0.5, M1...) is sufficiently refined for our purposes. We therefore coarsened Keenan & McNeil's classification. The adopted subtypes are given in the third column of Table 2. Keenan & McNeil's classification did not yield a perfect sequence as far as the behaviour of the near IR TiO bands is concerned. This can be due to variability, especially at the latest types. It is, however, also possible that the IR features do not behave exactly as the features in the blue region that are used classically. We reached a continuous sequence by adopting a slightly different spectral type for VY Leo.

K subtypes are not used consistently in the literature (Jaschek & Jaschek 1987). We adopted the subtypes K0, K1, K2, K3, K4, K5, and K7. For HD 90 362 which is classified K6 by Keenan & McNeil we adopted K7.

Strong nebular emission is present in many symbiotic systems and may contribute a noticeable fraction to the continuum radiation. This nebular radiation weakens the absorption of the TiO bands relative to the overall

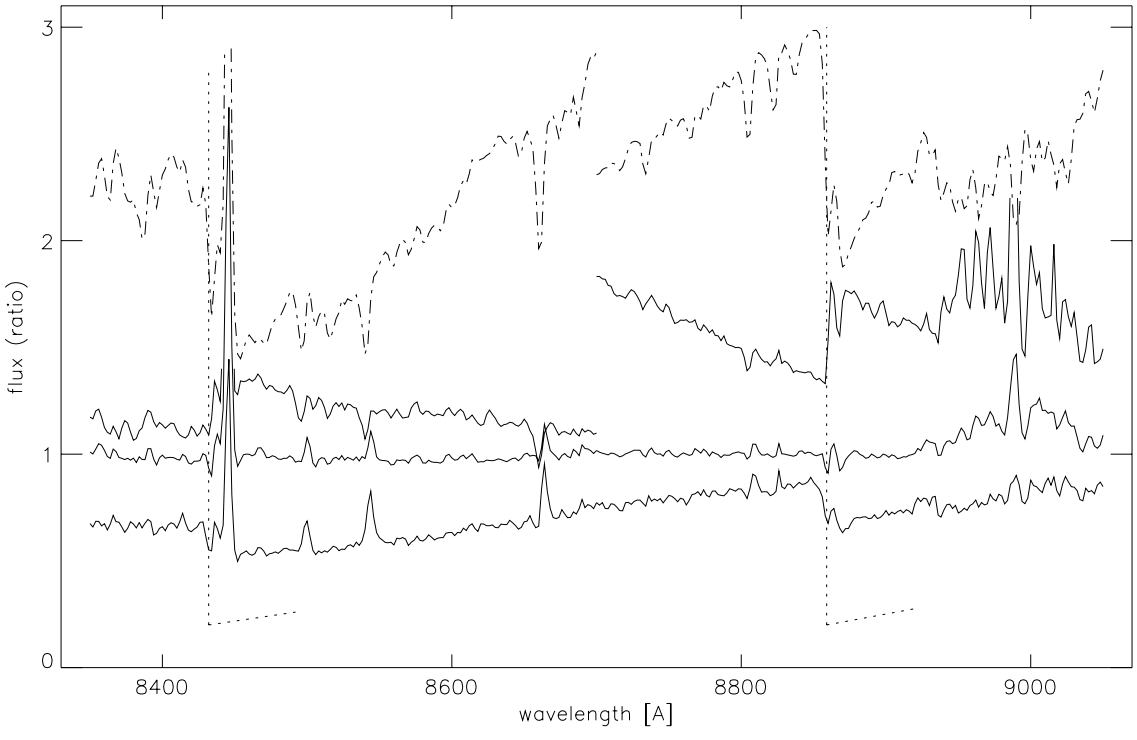

Fig. 2. The dashed-dotted line shows the spectrum of the symbiotic star Y CrA in the region of two TiO band heads (dotted lines). The full lines below show the spectrum of Y CrA divided by the spectra of standard stars of type M5 (lowest curve), M6 (middle), and M7 (top). For the purpose of comparison, all curves are arbitrarily scaled. Evidently, the TiO bands of Y CrA are not satisfactorily compensated by division by a M5 spectrum, while they are over-compensated with the M7 standard, and the best result is reached with the M6 standard. The strong features above 8950 Å are due to telluric absorptions

continuum and mimics an earlier spectral subtype. To avoid this source of error we had to correct the spectra of the symbiotic giants for the nebular contribution, before comparing them with the standard stars. The nebular continuum contribution, $F_{\rm neb}$, was determined from the equivalent width W(P14) of the H I Paschen emission line P14 λ8598. According to photoionization models (see e.g. Osterbrock 1989) nebular emission alone produces an equivalent width W(P14) $\approx$ 30 Å relative to the nebular continuum. Thus, the nebular continuum flux around λ8600 is $F_{\rm neb} = F_{\rm tot} \cdot W$(P14)/30 Å, where $F_{\rm tot}$ is the sum of the continuum fluxes of the nebula and the cool giant at this wavelength. In correcting the overall spectrum we neglected the spectral variation of the nebular continuum flux $F_{\rm neb}$, which is rather flat in the range of interest. In only a few cases, the correction for the nebular contribution altered the measured strength of the TiO bands noticeably.

Table 3 summarizes the classifications derived from the selected 5 TiO band heads. The objects are ordered according to their right ascension, like in the catalogues of Allen (1984) and Kenyon (1986). A long dash "—" means that the respective band is not visible because it is a) not present or too weak to be measured, b) not covered by the observations, c) evidently filled by nebular emission as the presence of bands at longer wavelengths indicates, or d) not measurable due to emission lines and insufficient resolution.

Table 2. Standard stars used in our comparison

Star	Spectral type according to Keenan & McNeil (1989)	Spectral type adopted for the present work
μ Hya	K4+ III	K4
HD 90 362	K6: IIIb	K7
61 Leo	M0 III	M0
θ Pyx	M0.5 III	M0.5
ν Vir	M1 III	M1
HD 107 003	M2 III	M2
74 Vir	M2.5 III	M2.5
ψ Vir	M3– III	M3
δ Vir	M3+ III	M3
HD 101 370	M3.5 III	M3.5
HD 80 431	M4 III	M4
HD 102 620	M4+ IIII	M4.5
HD 55 690	M5 III	M5
VY Leo	M5.5 III	M6
BK Vir	M7– III:	M7
SW Vir	M7 III:	M7
RX Boo	M7.5–M8	M7.5

None of the spectra of He2–104, He2–106, SSM1, and H1–36 shows absorption features that can be safely attributed to the cool star. Since He2–104, He2–106, and

Table 3. Spectral classification of the cool components in symbiotic systems according to the strength of 5 TiO band heads. "<" means "earlier than", for example

Object	Date	TiO band head					Adopted
		λ7054	λ7589	λ8432	λ8859	λ9209	classification
EG And	47 161	—	—	M3	—	—	M3
	47 508	—	—	M3	—	—	M3
AX Per	47 754	—	M3	≤ M3	M4	—	M3.5
	47 161	—	—	M5	—	—	M5
	47 508	—	—	M6	—	—	M6
	47 756	—	—	M4	—	—	M4
V741 Per	47 754	—	≤ K4	≤ M3	≤ M1	—	≤ K4
	47 508	—	—	≤ M3	—	—	≤ M3
BX Mon	48 697	M3	M5	M5	M5.5	M5.5	M5.5
	47 161	—	—	M4	—	—	M4
	47 507	—	—	M5	—	—	M5
MWC560	48 695	M3	M5.5	M5.5	M6	M5.5	M5.5
	49 473	M3	M5.5	M6	M6	M6	M6
Wray157	48 696	no TiO bands visible					≤ K4
	49 473	no TiO bands visible					≤ K4
RX Pup	48 695	no absorption features from the cool component					—
	49 473	—	—	—	M4	M7	M5.5
Hen160	48 696	M6	M7	M7	M7.5	M7	M7
	49 473	M3	M5.5	M7.5	M8	M7.5	M7
AS201	48 695	no TiO bands visible					≤ K4
	49 473	no TiO bands visible					≤ K4
He2–38	48 698	—	M3	M8	M7	M8	M7.5
	48 803	M3	M5	—	—	—	M5
	49 472	—	—	—	M6	—	M6
Hen461	48 698	M8	M7	M7	M7	M7	M7
SS29	48 696	no TiO bands visible					≤ K4
	49 472	no TiO bands visible					≤ K4
Hen653	48 696	M4.5	M7	M6	M5.5	M5.5	M6
SY Mus	48 696	M3	M4	M4	M4	≤ M5	M4
	48 804	M3.5	M5	—	—	—	M5
	49 472	M5	M5.5	M4.5	M5.5	≤ M5	M5
He2–87	48 698	—	M3.5	M5.5	M5.5	M7	M5.5
Hen828	48 698	M3	M5.5	M6	M5.5	M6.5	M6
Hen863	48 696	no TiO bands visible					≤ K4
St2–22	48 696	M3	M4	M4.5	M5.5	≤ M5	M4.5
CD–36.8436	48 697	M4.5	M5.5	M5.5	M5.5	M5.5	M5.5
Hen905	48 698	M2.5	M3	≤ M3	M3	≤ M5	M3
	49 473	M2	M3	M4	M3	≤ M5	M3.5
RW Hya	48 695	≤ M1	M1	≤ M3	M2.5	≤ M5	M2
	46 952	M1.5	M2	—	—	—	M2
	49 472	M1	M2	≤ M3	≤ M1	≤ M5	M2
Hen916	49 473	M3.5	M5	M5	M5	≤ M5	M5
V704 Cen	48 698	M7	M8	M6.5	M6.5	M5.5	M6.5
BD–21.3873	48 695	no TiO bands visible					≤ K4
	49 473	no TiO bands visible					≤ K4
He2–127	48 696	M3	M5.5	M6	M6	M5.5	M6
	48 804	—	M3.5	—	—	—	M3.5
	49 472	—	M3	—	M6.5	—	M5
Hen1092	48 698	M6.5	M6	M6	M6	M5.5	M6
	49 472	M5	M5.5	M5.5	M5.5	M6	M5.5
Hen1103	48 697	M3	M3.5	M3–M5	M3–M5	≤ M5	M3.5
	46 952	M3	M3.5	—	—	—	M3.5
HD 330 036	48 696	no TiO bands visible					≤ K4
	49 473	no TiO bands visible					≤ K4

Table 3. continued

Object	Date	TiO band head					Adopted
		λ7054	λ7589	λ8432	λ8859	λ9209	classification
He2–139	48 696	—	—	M6	M6	M7.5	M6.5
T CrB	47 377	—	—	M5	—	—	M5
	47 507	—	—	M4.5	—	—	M4.5
	47 664	—	—	M4.5	—	—	M4.5
AG Dra	47 754	≤ K3	—	—	—	—	≤ K3
	48 487	—	≤ K4	≤ M3	≤ M3	—	≤ K4
	47 377	—	—	≤ M3	—	—	≤ M3
	47 667	—	—	≤ M3	—	—	≤ M3
	47 756	—	—	≤ M3	—	—	≤ M3
W16–202	48 696	M3	M6	M5.5	M6	M5.5	M6
He2–147	48 697	—	M6	—	M7.5	M7.5	M7
Wray1470	48 697	M3	M3.5	M3–M5	M3	≤ M5	M3
He2–171	48 695	M3.5	M5.5	M7	M6.5	M7.5	M6.5
	49 472	—	—	M6	M6	M7.5	M6.5
Hen1213	48 697	no TiO bands visible					≤ K4
He2–173	48 696	M0	M3.5	M4.5	M5.5	≤ M5	M4.5
	46 953	M2	M4	—	—	—	M4
He2–176	48 697	M3	M3	M3	M3	≤ M5	M3
	49 473	—	M3	—	M6.5	M6.5	M5.5
Hen1242	48 698	M3	M5.5	—	—	—	M5.5
	49 472	M3	M5.5	M6	M6.5	M6	M6
HK Sco	48 698	M2	M3.5	M3	M3.5	≤ M5	M3.5
	49 473	M1	M3.5	M4	M4	≤ M5	M4
CL Sco	48 698	M3	M5	M4.5	M5	≤ M5	M5
V455 Sco	48 696	M3	M6	M6	M6.5	M7	M6.5
	49 473	M4	M6	M6	M7	M6	M6
Hen1341	46 952	K4–M1	M3.5	—	—	—	M3.5
	49 473	—	M3	M4.5	M5	—	M4
Hen1342	48 698	K4–M1	M0.5	≤ M3	≤ M1	≤ M5	M0.5
	46 952	K4–M0	K7	—	—	—	K7
	49 473	K4–M0	K7–M1	≤ M3	≤ M1	≤ M5	K7–M1
AS221	48 695	M3.5	M8	M7	M7.5	M7	M7.5
H2–5	49 473	M7	M6	M6	M5.5	≤ M5	M5.5
Hen1410	48 698	≤ K3	M2	≤ M3	≤ M1	≤ M5	M1.5
M1–21	46 953	M2.5	M5.5	—	—	—	M5.5
	49 473	M3	M5.5	M6	M6.5	M6.5	M6
Pt–1	46 953	M2	M3	—	—	—	M3
RT Ser	46 953	M4.5	—	—	—	—	M4.5
	49 473	M5	M6	M6	M6	M6	M6
AE Ara	46 952	M4	M5.5	—	—	—	M5.5
RS Oph	46 952	K4–M1	K4–M0	—	—	—	K4–M0
	47 756	—	—	≤ M3	—	—	≤ M3
AS255	48 698	no TiO bands visible					≤ K4
V2416 Sgr	48 696	M3	M6	M6	M7	M7	M6.5
	49 473	M3	M6	M6	M6	M6	M6
AS270	46 953	M4	M5.5	—	—	—	M5.5
H2–38	48 698	—	—	M8	M6.5	M8	M7.5
	49 472	—	—	—	M6	—	M6
SS129	48 698	≤ K3	K7–M1	≤ M3	≤ M1	≤ M5	K7–M1
V615 Sgr	48 698	M3	M5	M5.5	M5.5	M5.5	M5.5
Hen1591	48 698	no TiO bands visible					≤ K4
AS276	48 697	M3.5	M4.5	M4.5	M4.5	≤ M5	M4.5
V2506 Sgr	48 696	M4.5	M5.5	M5.5	M6	M5.5	M5.5
SS141	48 698	M4	M5.5	M5	M5.5	≤ M5	M5

Table 3. continued

Object	Date	TiO band head					Adopted
		λ7054	λ7589	λ8432	λ8859	λ9209	classification
AS289	47 664	—	—	M4	—	—	M4
	47 756	—	—	M3.5	—	—	M3.5
Y CrA	48 696	M5.5	M6	M6	M6	M5.5	M6
V2756 Sgr	48 697	K4–M1	M1	≤ M3	≤ M1	≤ M5	M1
YY Her	47 754	—	M4.5	M5	M3–M5	—	M4.5
	47 667	—	—	M3.5	—	—	M3.5
He2–374	48 698	M4.5	M5.5	M5.5	M5.5	M5.5	M5.5
AS296	47 664	—	—	M5	—	—	M5
AR Pav	48 698	M3	M4	M5	M5.5	≤ M5	M5
	46 953	M3	M5	—	—	—	M5
	49 472	M2	M5.5	M4.5	M5	≤ M5	M5
V443 Her	47 754	—	M5.5	M5.5	M5.5	—	M5.5
	47 377	—	—	M5.5	—	—	M5.5
	47 667	—	—	M5.5	—	—	M5.5
	47 756	—	—	M5.5	—	—	M5.5
V3811 Sgr	48 698	—	M2	M3–M5	M5	≤ M5	M3.5
AS316	48 698	—	M3.5	M3–M5	M4	≤ M5	M4
	48 805	M3.5	M4	—	—	—	M4
	49 473	M3	M3.5	M4	M4	≤ M5	M4
MWC960	46 952	≤ K3	K7	—	—	—	K7
AS327	48 698	M2.5	M3	M3	M3	≤ M5	M3
	48 805	K4–M2	M1	—	—	—	M1
FN Sgr	48 695	M2	M3	≤ M3	M3	≤ M5	M3
V919 Sgr	48 698	M2	M3.5	M3–M5	M5	≤ M5	M4
	46 952	M3	M4.5	—	—	—	M4.5
AS338	47 754	—	M2.5	≤ M3	M3	—	M3
	47 667	—	—	≤ M3	—	—	≤ M3
NSV11776	49 472	—	M5.5	M6	M7	M7.5	M7
Ap3–1	48 698	M4	M5.5	M5	M5	≤ M5	M5
BF Cyg	47 754	—	M2.5	M3.5	M4	—	M3.5
	47 507	—	—	M7	—	—	M7
	47 667	—	—	M4.5	—	—	M4.5
	47 756	—	—	M4.5	—	—	M4.5
CH Cyg	47 341	—	—	M7.5	—	—	M7.5
	47 667	—	—	M6.5	—	—	M6.5
Hen1761	48 698	M4	M5.5	M5	M5.5	M5.5	M5.5
	46 952	M5.5	M5.5	—	—	—	M5.5
HM Sge	47 754	—	—	> M6	—	—	> M6
	47 756	—	—	M7	—	—	M7
	49 472	—	—	—	—	M7	M7
AS360	47 754	—	M5	M5.5	M5.5	—	M5.5
	47 667	—	—	M4	—	—	M4
CI Cyg	47 754	M5	—	—	—	—	M5
	48 487	—	M5.5	M5.5	M6	—	M5.5
	47 377	—	—	M5	—	—	M5
	47 667	—	—	M5.5	—	—	M5.5
V1016 Cyg	48 486	—	—	> M6	—	—	> M6
	47 377	—	—	M6	—	—	M6
	47 507	—	—	M7	—	—	M7
	47 667	—	—	M7	—	—	M7
	47 756	—	—	M7.5	—	—	M7.5
RR Tel	48 696	M3	—	M7	M6.5	M8	M7
	b	M3	M3.5	—	—	—	M3.5
	49 472	—	—	M7	M6.5	M7	M7

Table 3. continued

Object	Date	TiO band head					Adopted
		λ7054	λ7589	λ8432	λ8859	λ9209	classification
PU Vul	47 754	—	M4.5	M6–M7	—	—	M5.5
	49 472	M3.5	M6	M7	M6.5	M7	M6.5
HBV475	47 754	M1–M3	—	—	—	—	M1–M3
	48 488	—	M5.5	M6–M7	M6.5	—	M6
	47 377	—	—	M5.5	—	—	M5.5
	47 508	—	—	M6	—	—	M6
	47 667	—	—	M6	—	—	M6
	47 756	—	—	M7	—	—	M7
CD–43.14304	48 698	no TiO bands visible					$\leq$ K4
	48 804	no TiO bands visible					$\leq$ K4
	49 472	no TiO bands visible					$\leq$ K4
S190	47 754	—	$\leq$ K4	$\leq$ M3	$\leq$ M1	—	$\leq$ K4
	47 667	—	—	$\leq$ M3	—	—	$\leq$ M3
	49 473	no TiO bands visible					$\leq$ K4
AG Peg	47 754	—	M3	$\leq$ M3	M2.5	—	M3
	47 377	—	—	M3	—	—	M3
	47 756	—	—	M3	—	—	M3
Z And	47 754	M3.5	—	—	—	—	M3.5
	48 488	—	M3.5	M4.5	M3.5–M5	—	M4
	47 161	—	—	M5	—	—	M5
	47 377	—	—	M5	—	—	M5
	47 508	—	—	M4	—	—	M4
	47 756	—	—	M4	—	—	M4
R Aqr	47 161	—	—	M8	—	—	M8

H1–36 show photometric variations and dust emission in the IR typical of mira type stars (Whitelock 1987) they should contain a rather late M-type giant. Therefore, we suppose that in these four systems the cool star is obscured by dust, so that its light cannot compete with the nebular emission. Very little is known about SSM1.

Spectral types from different TiO bands. In Fig. 3 we compare the spectral types derived from the different TiO band heads. It is apparent that the spectral classification derived from the TiO band λ7054 is systematically shifted by about two spectral subclasses towards earlier types, when compared with the TiO bands at longer wavelengths. The bands $\lambda\lambda$7589, 8432, 8859, and 9209 correlate very well. Already Kenyon & Fernández-Castro (1987) had noticed that the molecular absorptions at shorter wavelengths mimic earlier spectral types for the giants in symbiotic systems. The observed inconsistency is possibly explained by assuming significant contamination of the λ7054 TiO band by nebular emission. The bands at longer wavelengths are expected to be much less affected due to the rapid increase in brightness of the red giant towards the IR.

For the final classification given in the last column of Table 3, we "averaged" the results from the TiO bands $\lambda\lambda$7589, 8432, 8859, and 9209. Due to the above described effect, the band at λ7054 is only considered where the other bands are not available.

3.2. Comparison with published classifications

In Fig. 4 we compare our classification with publications that contain a certain number of objects in common with us. The top panel shows that our results correlate well with those of Kenyon & Fernández-Castro (1987) and Schulte-Ladbeck (1988). Their classifications differ on average less than 0.8 spectral subtypes from ours. We take this as a measure for the reliability of our classification. Note that non-negligible differences have to be expected due to the intrinsic spectral variability of mira systems. The spectral types of a few systems may also be affected by outbursting hot components which may lower unexpectedly the absorption contrast of the molecular absorptions (see Sect. 3.3). Further, we cannot exclude the possibility of small variationes ($<$ 1 subclass) due to e.g. irradiation or tidal effects. The good agreement with Schulte-Ladbeck (1988) is not so surprising as she employed a similar technique and similar spectral data as in this work. Kenyon & Fernández-Castro (1987) employed for their classification work molecular bands between 6000 Å and 8000 Å. They noticed, as in this work, the veiling problem in the shorter wavelength bands. The good agreement with our work indicates that their careful consideration of this problem

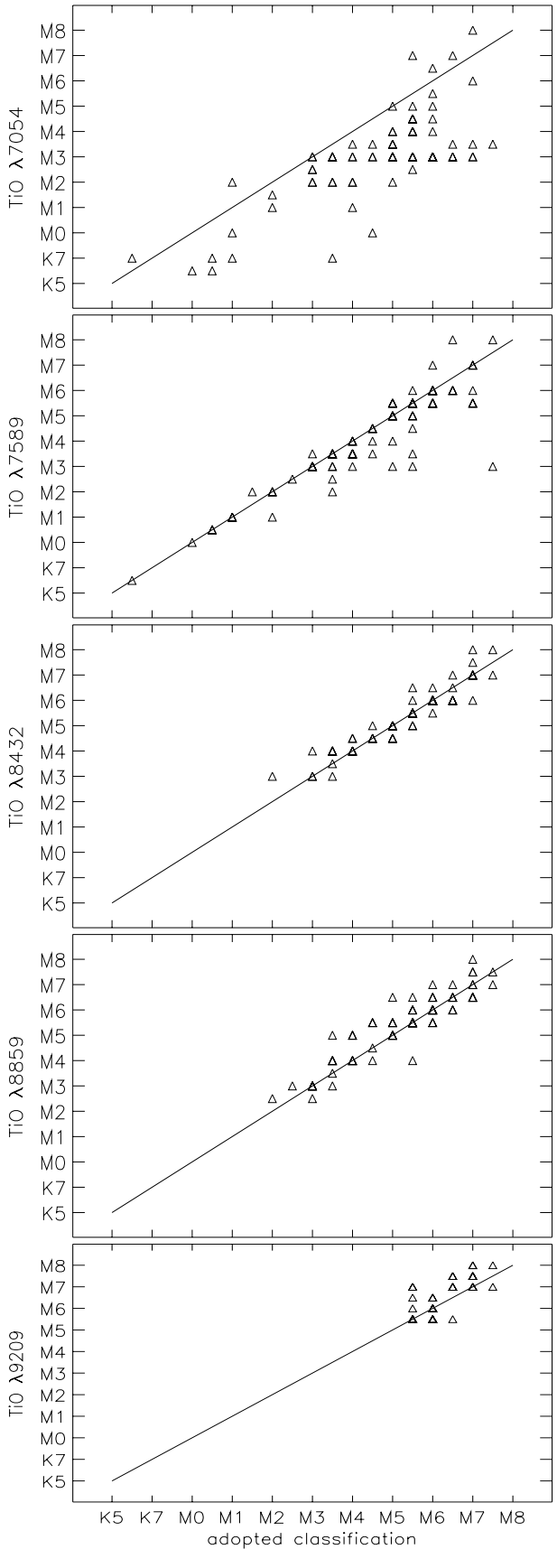

Fig. 3. Comparison of the adopted classification and that suggested by the different TiO band heads

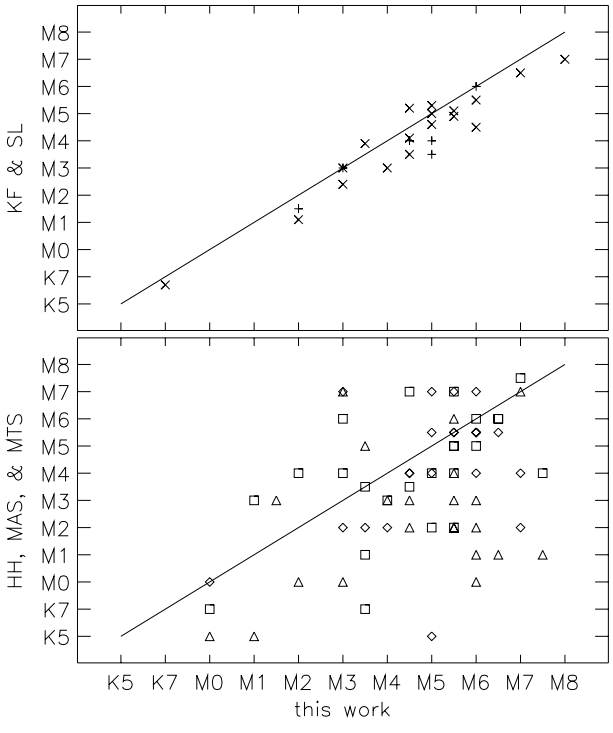

Fig. 4. Comparing our spectral types with the five most extended classification works in the literature. Top panel: comparison with Kenyon & Fernández-Castro (1987, ×) and Schulte-Ladbeck (1988, +); bottom: comparison with Medina Tanco & Steiner (1995, □), Harries & Howarth (1996, ♢), and Mikołajewska et al. (1997, △)

overcame the disadvantage of using a spectral range that does not reach very far into the IR.

The results of Medina Tanco & Steiner (1995), Harries & Howarth (1996), and Mikołajewska et al. (1997) differ significantly from ours in the average by roughly 2 subclasses (Fig. 4). These authors based their classification mainly on spectral features at shorter wavelengths and/or used insufficient spectral resolution. Presumably, the scatter in the bottom panel of Fig. 4 is at least partly caused by the veiling problem for red giants in symbiotic systems as discussed previously. The tendency of spectral types towards an earlier classification supports this interpretation.

3.3. Temporal variability

Several systems have been observed more than once. This allows to search for spectral variations. We can detect variability only in systems with strong changes exceeding two spectral subtypes. We find in Table 3 seven such variable systems, namely AX Per, He2–38, He2–127, BF Cyg, RR Tel, and HBV 475.

The systems He2–38, He2–127, and RR Tel contain mira variables as cool giants (see Whitelock 1987) and changes of the spectral type related to pulsation are therefore expected.

Table 4. Systems with spectral types earlier than K5

Object	Date	Adopted classification
V741 Per	47758	G5
Wray 157	49472/3	G5
AS201	49472/3	G5
BD–21.3873	49472/3	K2
HD 330 036	49472/3	G5
AG Dra	47758	K2
He2–467	47758	K0
CD–43.14304	49472/3	K7
S190	49472/3	G5
	47758	G5

The spectra of AX Per and BF Cyg were taken during a Z And-type outburst phase. A comparison with V-band light curves of AX Per and BF Cyg from the AFOEV (Association Francaise des Observateurs d'Étoiles Variables) reveals a correlation between the spectral type and the system brightness. We obtained for AX Per a spectral type of M5 at magnitude $m_V = 11\overset{\mathrm{m}}{.}5$, M6 at $m_V = 10\overset{\mathrm{m}}{.}5$, but M3.5 and M4 during maximum brightness ($m_V = 9\overset{\mathrm{m}}{.}5$). Similarly, we find M7 for BF Cyg at $m_V = 11\overset{\mathrm{m}}{.}8$, M4.5 at $m_V = 11\overset{\mathrm{m}}{.}0$, and M3.5 and M4.5 near maximum ($m_V = 10\overset{\mathrm{m}}{.}4$). Thus, we registered weaker TiO band absorptions during outburst. This effect can be explained by the additional continuum contribution of the hot (outbursting) companion, which lowers the absorption contrast of the TiO bands. Another explanation is that the hot star heats up the red giant atmosphere. However, this effect cannot be very strong as no significant changes in the IR bands of the cool giant are seen during such outbursts (e.g. Munari et al. 1992). It is interesting to note that also Kenyon & Fernández-Castro (1987) found for a given symbiotic system weaker absorptions (i.e. earlier spectral types) when the target was bright.

The variations we find for HBV475 are probably not real. The much earlier spectral type (M1 − M3) obtained for the run on JD 47754 (see Table 5) is most likely a spurious result. The reason is the limited resolution of that spectrum ($\Delta\lambda = 15$ Å), which fails to resolve the stellar absorptions from the rich and strong emission line spectrum of HBV475. Note that we derived a spectral type of M7 from a higher resolution spectrum ($\Delta\lambda = 2$ Å) taken just two days later. This example is a clear warning that spectral types from lower resolution spectra have to be considered cautiously. In our case, this concernes the run at JD 47754.

We conclude that significant and real changes in the cool giant's spectral type are seen only in systems containing mira variables. Our data set is, however, not sufficiently homogeneous and systematic to search for small spectral type variations (≤ 1 spectral subtype) intrinsic to the cool giant, which may be caused by e.g. irradiation effects, tidal interaction or outburst activity.

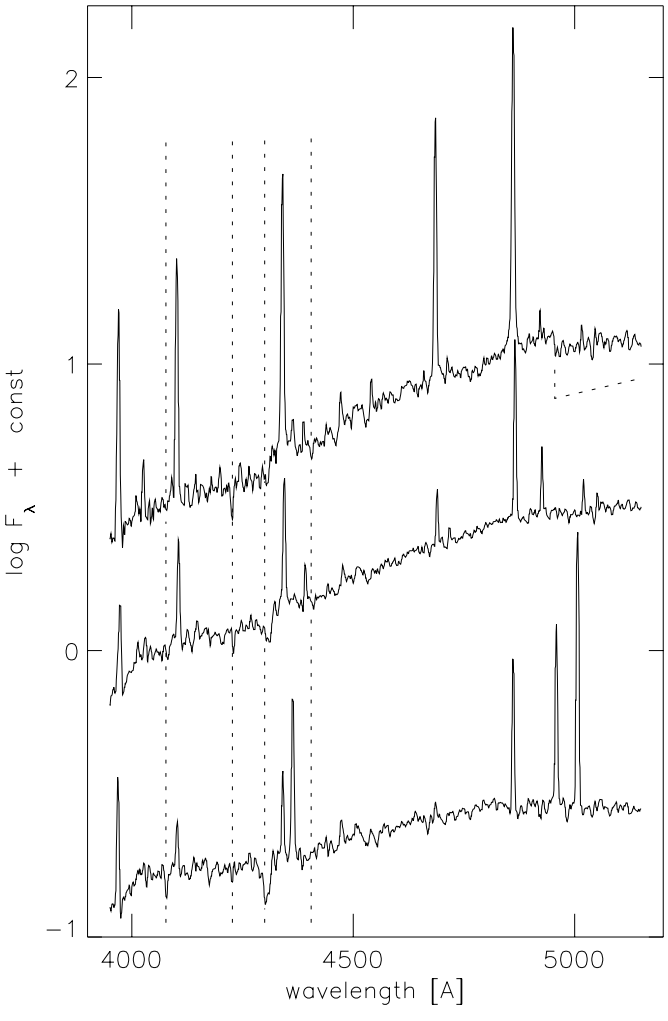

Fig. 5. The blue spectra of AS201 (bottom), BD–21.3873 (middle), and CD–43.14304 (top). The dashed lines mark the absorption lines Sr II λ4077, Ca I λ4227, CH λ4300, and Fe I λ4405. In addition, the TiO λ4955 band head is marked in the spectrum of CD–43.14304

3.4. Classification of the yellow symbiotics

The spectral classification based on near IR TiO bands fails for cool giants with spectral types earlier than K5. For these objects we analyze spectra taken in the blue wavelength region.

Fortunately, the observed G and K giants are sufficiently bright in the blue wavelength region, such that the veiling by the nebular continuum emission can be neglected. Thus we can use the known line ratio criteria for the spectral classification (Keenan & McNeil 1976; Yamashita et al. 1977; Jaschek & Jaschek 1987). However, the blue spectra of the symbiotic giants are still contaminated by strong emission lines, mainly H and He recombination and nebular [O III] emission lines (see Fig. 5). This prevents particularly the use of criteria based on hydrogen lines. Due to the moderate resolution of our spectra, we are additionally limited to strong spectral features.

Table 5. Spectral types of the cool components of symbiotic stars

Object	IR–type	Spectral type		
		this work	litera–ture	refe-rence
EG And	s	M3		
SMC1	s		C3,2	MSV
SMC2	s		K	MSV
SMC3	s		K–M	MSV
SMC N60	s		C3,3	MSV
SMC Ln358	s		K	MSV
SMC N73	s		K7	MSV
AX Per	s	M4.5		
V741 Per	d′	G5		
S32	s		C1,1CH	S
UV Aur	d′		C	KF
LMC S154	d		C2,2	MSV
LMC S147	s		M1	MSV
LMC N19	s		M4	M
LMC1	d		C4,3	MSV
LMC N67	s		C3,2	MSV
Sanduleak's star	d:			
LMC S63	s		C2,1J	MSV
BX Mon	s	M5		
MWC560	s	M5.5		
Wray157	d′	G5		
RX Pup	d	M5.5		
Hen160	s	M7		
AS201	d′	G5		
He2–38	d	M6		
Hen461	s	M7		
SS29	s	$\leq$ K4		
Hen653	s	M6		
SY Mus	s	M4.5		
BI Cru	d		M0–M1	SL
RT Cru			M4–M5	CSJ
He2–87	s	M5.5		
Hen828	s	M6		
SS38	d	C		
Hen863	s	$\leq$ K4		
St2–22	s	M4.5		
CD–36.8436	s	M5.5		
V840 Cen	s		K5	DS
Hen905	s	M3		
RW Hya	s	M2		
Hen916	s	M5		
V704 Cen	d	M6.5		
He2–104	d			
He2–106	d		$\geq$ M5	SL
V417 Cen	d′		G8–K2	CES
BD–21.3873	s	K2		
He2–127	d	M5		
Hen1092	s	M5.5		
Hen1103	s	M3.5		
HD 330 036	d′	G5		
He2–139	d	M6.5		
T CrB	s	M4.5		
AG Dra	s	K2		

Object	IR–type	Spectral type		
		this work	litera–ture	refe-rence
W16–202	s	M6		
He2–147	d	M7		
UKS Ce1	s		C4,5Jch	S
Wray1470	s	M3		
He2–156	s		K5	MAS
He2–171	d	M6.5		
Hen1213	s	$\leq$ K4		
He2–173	s	M4.5		
He2–176	d	M4		
Hen1242	s	M6		
AS210	d	C		
HK Sco	s	M3.5		
CL Sco	s	M5		
MaC1–3	d		M2	MAS
V455 Sco	s	M6.5		
Hen1341	s	M4		
Hen1342	s	M0		
AS221	s	M7.5		
H2–5	s	M5.5		
Sa3–43	s		M	A84
Th3–7	s		M3	MAS
DracoC–1			C	ALS
Th3–17	s		M3	MAS
Th3–18	s		M2	MAS
Hen1410	s	M1.5		
V2116 Oph	s		M6	DMB
Th3–29	s		M3	MAS
Th3–30	s		M1	MAS
Th3–31	s		M5	A80
M1–21	s	M6		
He2–251	d		$<$ K5	CES
Pt–1	s	M3		
RT Ser	s	M6		
AE Ara	s	M5.5		
SS96	s		M0	MTS
W16–294	s		K5	MAS
WR99	s			
UU Ser	s		M4	MAS
AS239	d		M	A78
AS241	s		M1	MAS
SSM1	s			
Hen1481	s			
He2–275	s		M3	MAS
H1–36	d		M4	MTS
W16–312	d			
Th4–4	s		M	A84
RS Oph	s	K7		
AS245	s		M2	MAS
He2–294	s		M3	MAS
Bl3–14	s		M6	A80
Bl3–6	s		M3	MAS
Bl L	s		M6.5	A80
ALS2	s		M2	MAS
AS255	s	$\leq$ K4		

Table 5. continued

Object	IR–type	Spectral type		
		this work	litera–ture	refe-rence
V2416 Sgr	s	M6		
MaC1–9	s		M2	MAS
SS117	s		M5	MTS
DT Ser			G–K	CSJ
Ap1–8	s		M4	MAS
SS122	d		M7	MTS
AS270	s	M5.5		
H2–38	d	M7		
AS269				
SS129	s	M0		
V615 Sgr	s	M5.5		
Hen1591	d′	$\leq$ K4		
Ve2–57	s			
AS276	s	M4.5		
Ap1–9	s		K5	MAS
AS281	s		M5.5	HH
V2506 Sgr	s	M5.5		
SS141	s	M5		
AS280	s			
AS289	s	M3.5		
Y CrA	s	M6		
V2756 Sgr	s	M1		
HD319 167	s		M3	MAS
YY Her	s	M4		
He2–374	s	M5.5		
AS296	s	M5		
NSV10453			M	CES
AS295B				
AR Pav	s	M5		
He2–376	s		M2	MAS
Hen1674	s		M5	MTS
AS299	s		M0	MAS
He2–390	d		M1.5	MTS
V443 Her	s	M5.5		
V3804 Sgr	s		M5	MTS
AS304	s		M4	A80
V2601 Sgr	s		M5	MAS
V3811 Sgr	s	M3.5		
AS316	s	M4		
K3–9	d		M3	MAS
MWC960	s	K7		
AS323	s		M3	MAS
AS327	s	M2		
FN Sgr	s	M3		
Pe2-16	s		K5	MAS
V919 Sgr	s	M4.5		
CM Aql	s		M0	
AS338	s	M3		
NSV11776		M7		
Ap3–1	s	M5		
MaC1–17	s		M1	MAS
V352 Aql	s		M3	MAS
ALS1	s		M3	MAS
BF Cyg	s	M5		
CH Cyg	s	M7		
Hen1761	s	M5.5		
HM Sge	d	M7		
DQ Ser			M	CSJ
AS360	s	M5		
CI Cyg	s	M5.5		
V1016 Cyg	d	M7		
RR Tel	d	M6		
PU Vul	s	M6		
He2–467	s	K0		
He2–468	s		M	A84
HBV475	s	M6		
CD–43.14304	s	K7		
V407 Cyg	d		M6	MMS
S190		G5		
AG Peg	s	M3		
Z And	s	M4.5		
R Aqr	d	M8		

References: A78: Allen (1978); A80: Allen (1980); A84: Allen (1984); ALS: Aaronson et al. (1982); CES: Cieslinski et al. (1994); CSJ: Cieslinski et al. (1998); DMB: Davidsen et al. (1977); DS: Duerbeck & Seitter (1989); KF: Kenyon & Fernández-Castro (1987); HH: Harries & Howarth (1996); M: Morgan (1996); MAS: Mikołajewska et al. (1997); MMS: Munari et al. (1990); MSV: Mürset et al. (1996); MTS: Medina Tanco & Steiner (1995); S: Schmid (1994); SL: Schulte-Ladbeck (1988).

In view of these restrictions we confined our classification to the spectral types G0, G5, K0, and K2 similar to the system of the HD catalogue. As main classification criteria we use the G band, which is strongest for G5, Ca I λ4227, which increases steadily from G0 to K7, and Fe I λ4405 which is only strong in K types. In addition we consider also the absorption features of Fe I, Sr II, and other species as secondary indicators. Because our classification relies relatively strongly on the CH band we point out that our classification may be inaccurate for stars with peculiar abundance patterns (e.g. carbon rich or carbon deficient objects).

In our sample we identify a very homogeneous group consisting of V741 Per, Wray157, AS201 and S190. All of them exhibit a very strong CH-band and relatively weak lines from Ca I and Fe I. Therefore we assign to them a spectral type of G5. HD 330 036 exhibits a very similar absorption spectrum except for the CH-band which is

substantially weaker than in the previous group. From the Fe I, Ca I and Sr II lines alone and assuming that the weak CH-band is due to an abundance anomaly we adopt for this star as well a spectral type of G5.

BD–21.3873 and AG Dra have a relatively weak CH-band and strong features of Ca I and Fe I λ4405 compatible with a K2 classification. In the spectrum of He2–467 the Fe I lines are stronger than in AG Dra or BD–21.3873 while Ca I λ4226 is rather weak. Again, this could be an abundance effect as both, BD–21.3873 and AG Dra are known to be metal poor objects (Smith et al. 1996, 1997). Based on these considerations we assign a spectral type K0 to He2–467. In the spectrum of CD–43.14304 we see clearly a weak TiO absorption band at λ4955. This suggests a spectral type of K7 in contradiction to the type listed in Table 3.

3.5. Symbiotic carbon stars

S32, AS210, and SS38 show strong CN absorptions bands which indicate unambiguously that they contain a cool giant of spectral type C. For carbon stars the strength of the molecular bands depends not only on the photospheric temperature but also strongly on the carbon abundance (e.g. Keenan & Morgan 1941; Yamashita 1972). Because we do not possess the respective standard star spectra we abstain from a detailed classification. Nonetheless, the overall spectra indicate that the giant in S32 is an early C star (see also Schmid 1994), while AS210 and SS38 contain late C stars, which are probably mira variables (Whitelock 1987).

4. Catalogue of spectral types for the cool giants in symbiotic systems

In Table 5 we present a catalogue of spectral types for the cool components in symbiotic systems. The catalogue is mainly based on our classifications described in the previous Section. For those objects where we found different spectral types for different observations, we entered in Table 5 the "average". For objects not covered by our own observations we adopt published spectral types when available. We believe most literature classification to be less accurate than our own, the exceptions being the spectral types from Schulte-Ladbeck (1988) and Kenyon & Fernández-Castro (1987) (see the discussion in Sect. 3.2). The catalogue contains 179 entries, of which 172 objects have a spectral classification for the cool giant. In this work, we classified 97 objects, many for the first time.

The catalogue includes the following objects:

- all systems contained in the catalogue of Allen (1984), including the "possible symbiotic stars";
- all additional objects listed in Mikołajewska et al. (1997);
- the systems identified by Cieslinski et al. (1994, 1997, 1998);
- all systems in the Magellanic Clouds included in the Paper by Mürset et al. (1996);
- in addition: MWC560 (Michalitsianos et al. 1991), S32 and S190 (Downes & Keyes 1988), and LMC N19 (Morgan 1996).

We did not attempt to present a complete list of all objects claimed to be symbiotic in the literature since we suppose that some identifications would require closer reinspection which is beyond the present scope.

The catalogue gives also the classification into s-, d-, and d′-types according to the IR colors (see Webster & Allen 1975; Allen 1982). The s-types show in the IR a normal continuum of a cool giant, while d- and d′-types show strong dust emission. The s-types contain non-variable red giants and typically have binary periods of $P \approx 1-3$ years. d-type systems probably all contain a mira variable as cool component and have probably very long orbital periods $P > 20$ yr. The d′-types have several special properties, the most conspicuous of which is the presence of a F- to early K-type giant instead of a cooler star.

The IR classifications given in Table 5 are adopted from Allen (1984), Mikołajewska et al. (1997), and Mürset et al. (1996), with a few exceptions: V417 Cen was classified d′ by Van Winckel et al. (1994). He2–147 is of type d according to Whitelock (1987). Hen1591 is classified as d-type by Allen (1984); however, in view of the early spectral type d′ seems to be more appropriate. In the catalogue there are 133 s-types, 30 d-types, 7 d′-types and 9 objects with no IR classification.

5. Distribution of spectral types

It is instructive to compare the distribution of spectral types of the cool giants in symbiotic systems and that of giants in the solar neighbourhood. For this we restrict our sample to galactic objects, thus excluding the 13 Magellanic Cloud systems and Draco C–1. A discussion of the spectral types of the cool giants in the Magellanic Cloud systems in relation to galactic systems can be found in Mürset et al. (1996).

5.1. Normal M–giants versus miras and other types

Among the 165 galactic objects we count 129 M-type stars, including 27 d-type systems. There are 15 s-type and 5 d′-type systems with a spectral type earlier than M. Further we have 3 systems with late type carbon stars (UV Aur, SS38, and AS210) and 2 systems with early type carbon stars (UKS–Ce1, S32). From these figures we conclude:

- Spectral types: 80% of the objects contain a M or late C star, which indicates that symbiotic giants have a

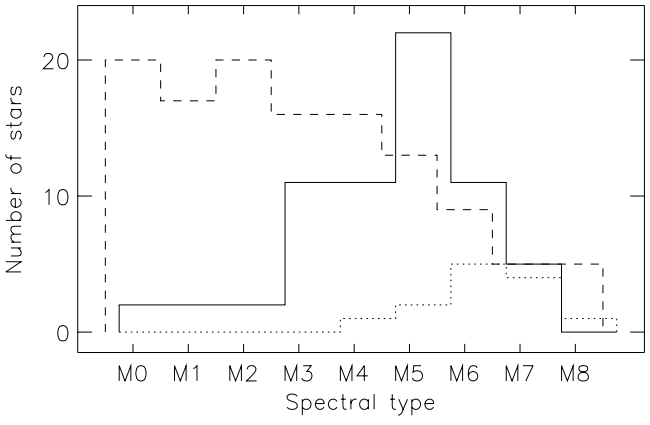

Fig. 6. Frequency of the M–subtypes among the cool components of s-type symbiotic systems (full line) and d-types (dotted) according to Table 6The dashed line shows the distribution of M giants in the HIPPARCOS catalogue

very late spectral type. A substantial fraction of the earlier types seems to belong to the halo population (e.g. Schmid & Nussbaumer 1993; Smith et al. 1996, 1997), implying that they constitute a distinct subclass of the symbiotics.

- Variability: the relative frequency of mira type stars is much larger among symbiotic giants than among the giants of the solar neighbourhood. While only 3 out of the 122 giants in the HIPPARCOS sample (to be discussed in the next Section) are mira variables, 27 symbiotics (= 16%) are d-types which probably all contain a mira.
- Chemical peculiarities: With 5 out of 167 the fraction of carbon rich symbiotic systems is comparable to the ratio between C and M giants in the solar neighbourhood. It is well known that the number ratio of C to M field giants is much higher in the Magellanic Clouds than in the Galaxy (e.g. Blanco et al. 1978). Correspondingly, a much larger C-star fraction among the symbiotic systems was obtained for the Magellanic Clouds by Mürset et al. (1996), who found 6 carbon-rich systems out of the 11 objects that could be classified. Thus, the frequency of carbon-rich symbiotic systems seems to reflect just the number ratio of C to M giants of the parent galaxy.
  Barium-star type abundance anomalies are measured or strongly suspected in the four systems S32, UKS–Ce1, AG Dra and BD–21.3873 (see Schmid 1994; Smith et al. 1996, 1997). There is no S-star known in a symbiotic system.

5.2. Distribution of M-subtypes

Figure 6 displays the distribution of M-type giants in 79 symbiotic systems based on our classifications given in the third column of Table 5. Classifications from the literature are not included in order to have a homogenous data set. Figure 6 emphasizes the differences between d- and s-types. The spectral class distribution of the d-types peaks around M6 about one subclass later than for the s-types. We found no red giant with a spectral type earlier than M4 in a dust-rich system. The differences in the spectral type distribution of s- and d-types reflects the basic property of the IR classification, which segregates the more evolved, high mass-loss giants in the d-type systems from the s-types which contain less extreme giants.

5.2.1. M-subtypes in the solar neighbourhood

The distribution of spectral types of M-giants in the solar neighbourhood $d < 150$ pc is derived from the HIPPARCOS catalogue (ESA 1997). A sample of M giants was selected according to the following HIPPARCOS parameters: large parallax ($\pi > 6.667$ mas), red colors ($V - I > 1\overset{\mathrm{m}}{.}5$), spectral classification M, and large intrinsic brightness ($M_{Hp} = Hp + 5\log(\pi[\mathrm{mas}]) - 10^{\mathrm{m}} < 3^{\mathrm{m}}$). Hp is the mean magnitude in the broad band HIPPARCOS filter. This criterion separates the giants from the dwarfs. It also ensures a very high degree of sample completeness and helps to avoid that faint and probably more distant objects with large parallax errors enter the sample. According to these criteria we found 122 objects.

Before proceeding, we performed various tests to check for sample completeness. We found only one object, the mira variable R Cas (HIP118188), with a parallax of 9.4 mas, which failed to fulfill the above criteria. The reason is the inappropriate Hp-magnitude for this large amplitude variable with a magnitude range from $5\overset{\mathrm{m}}{.}1 - 9\overset{\mathrm{m}}{.}3$. The Hp-magnitude is a median magnitude of all HIPPARCOS photometric measurements. Due to unfortunate sampling of the R Cas light curve the mean value $Hp = 8\overset{\mathrm{m}}{.}7$ is close to the minimum brightness and the corresponding absolute magnitude does not conform with the $M_{Hp} < 3^{\mathrm{m}}$ limit. In the following we include also this object in our sample. Further we excluded two objects, an M-supergiant (α Ori), and a faint M-giant without spectral subtype (M...) and large parallax error. Thus there remain 121 M-giants in the sample.

This sample includes 11 objects with variability flag 3 in the HIPPARCOS catalogue, which indicates large amplitude ($\Delta Hp > 0\overset{\mathrm{m}}{.}6$) variables. 3 out of these 11 objects are in fact mira-variables, namely o Cet, R Leo and R Cas (see also van Leeuven et al. 1997). Most of the other objects in this variability group are classified as semi-regular variables.

The distribution of spectral subtypes among the selected M-giants is shown in Fig. 6. For classifications with half subclasses (e.g. M3/4 III), we have chosen alternatively the earlier or the later full subclass. Median spectral types are adopted for the two mira variables o Cet and R Leo, for which the catalogue gives a range in spectral type (e.g. M5 − M9 = M7).

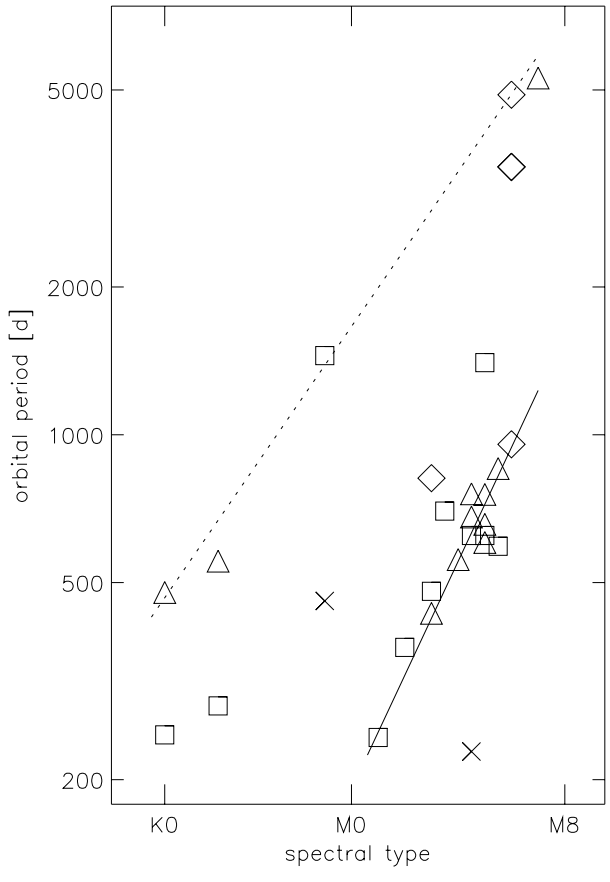

Fig. 7. Orbital periods as a function of the spectral type of the cool binary components. The symbols denote different activity classes: recurrent novae (×), variables with Z And type outbursts (△), symbiotic novae (◇), and objects without recorded strong outbursts (□). The full line markes the period limit discussed in the text, the dashed line connects the relatively widest systems

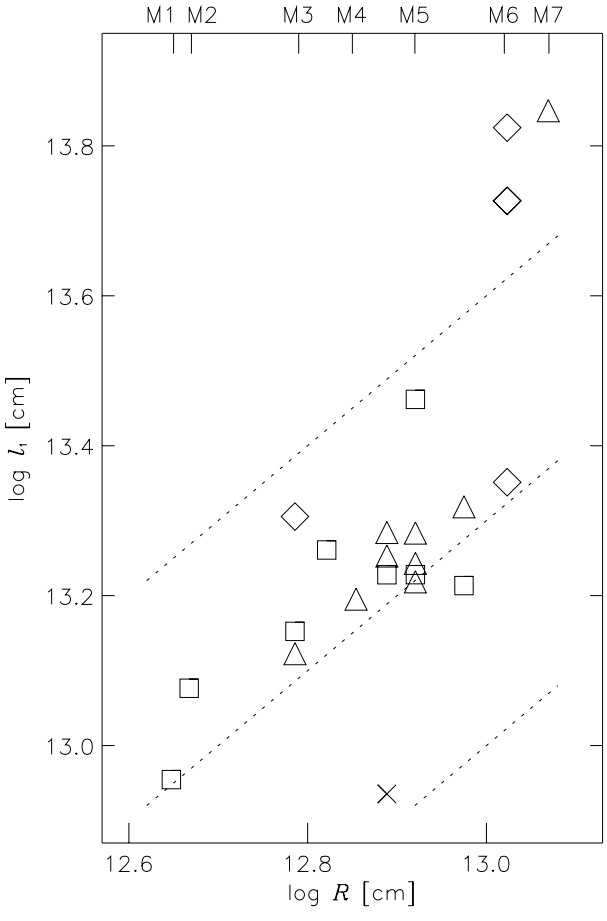

Fig. 8. The distance of the inner Lagrangian point, ℓ_1, versus the cool star's radius, R, as determined from the spectral type, for M-type systems. Symbols are as in Fig. 7. The dotted lines denote $\ell_1 = R$, $\ell_1 = 2 \cdot R$, and $\ell_1 = 4 \cdot R$, respectively

5.2.2. Symbiotic giants vs. field giants

Figure 6 shows that the distribution of spectral types for the cool giants in symbiotic systems (present classifications only) differs strongly from the distribution of field giants in the solar neighbourhood. As already noticed by Allen (1980), there exists in symbiotic systems a very strong bias in favour of late spectral types ($\geq$ M5) when compared to the field giants. With our improved and more comprehensive classification we find an even stronger bias than Allen discovered. The number ratio between late ($\geq$ M5) and early ($<$ M5) type M giants is 1.7 for the giants in symbiotic systems but only 0.36 for the giants in the solar neighbourhood. Late M-stars and mira-type variables exhibit larger radii and much stronger mass loss than early M giants. Large radius and high mass loss for the cool component are possibly key ingredients for triggering symbiotic activity on a white dwarf companion. We suggest that this could explain the high frequency of late M giants and mira variables among symbiotic giants.

6. Spectral type and orbital period

For M giants, the spectral type is strongly correlated with mass loss, temperature, and radius (see e.g. Reimers 1975; Dyck et al. 1996; Dumm & Schild 1998). Stellar radius and mass loss are known to be key parameters for triggering interaction phenomena in binaries. As we have now a large sample of accurate spectral types for the cool giants in symbiotic systems at hand we can search for correlations with binary parameters and outburst properties.

We searched the literature for orbital parameters. We found orbital periods for about 30 systems whereas additional parameters are less frequently determined. The periods are listed in Table 6. About half of the periods are determined from radial velocity measurements, the other half is deduced from periodic brightness variations that are supposed to be due to the binary revolution (see also Mikołajewska 1997).

In Fig. 7 we plot the periods from Table 6 versus the respective spectral types from Table 5. The shortest period system, at the lower right corner of the plot, is the symbiotic recurrent nova T CrB. T CrB is an extra-ordinary

Table 6. Published orbital periods of symbiotic systems. The activity classes are labeled in the following way: ClSS = Z And type outbursts (classical symbiotic variables); SyNe = symbiotic novae; SyRNe = recurrent novae; stable = no strong outburst is recorded (to our knowledge)

Star	Activity class	P [d]	Reference
EG And	stable	481.1	Munari (1993)
AX Per	ClSS	680.8	Mikołajewska & Kenyon (1992a)
S32	stable	612	Dumm et al., in preparation
BX Mon	stable	1401	Dumm et al. (1998)
SY Mus	stable	624.5	Pereira et al. (1995)
RW Hya	stable	370.2	Kenyon & Mikołajewska (1995), Schild et al. (1996)
V417 Cen	stable	246.68	Van Winckel et al. (1994)
BD–21.3873	stable	281.6	Smith et al. (1997)
T CrB	SyRN e	227.53	Kenyon & Garcia (1986)
AG Dra	ClSS	554	Meinunger (1979)
HK Sco	stable	700:	Swope (1941)
CL Sco	stable	624.7	Kenyon & Webbink (1984)
RT Ser	SyNe	3497	Pavlenko et al. (1996)
RS Oph	SyRNe	460	Dobrzycka & Kenyon (1994)
V2756 Sgr	stable	243	Hoffleit (1970)
YY Her	ClSS	558	Rejkuba et al. (1997)
AS296	ClSS	658	Munari et al. (1995)
AR Pav	ClSS	604.5	Mayall (1937), Bruch et al. (1994)
V443 Her	stable	594	Dobrzycka et al. (1993), Kolotilov et al. (1995a)
V2601 Sgr	stable	850:	Hoffleit (1968)
AS338	ClSS	434.1	Munari (1992)
BF Cyg	ClSS	756.8	Pucinskas (1970), Mikołajewska et al. (1989)
CH Cyg	ClSS	5294	Hinkle et al. (1993)
CI Cyg	ClSS	854	Kenyon et al. (1991)
PU Vul	SyNe	4918	Kolotilov et al. (1995b)
He2–467	ClSS	478.5	Arkhipova et al. (1995)
HBV475	SyNe	956.5	Schild & Schmid (1997)
CD–43.14304	stable	1448	Schmid et al. (1998)
AG Peg	SyNe	816.5	Fernie (1985), Kenyon et al. (1993)
Z And	ClSS	758.8	Mikołajewska & Kenyon (1996a)

symbiotic, and we will discuss it further below. Neglecting this object for the moment, we discover that the systems that contain an M giant cluster in Fig. 7 on a straight line. While there are some system above this line, there is none far below. Therefore, the line represents a minimum orbital period, $P_{\rm min}$, for symbiotic systems of a given spectral type. The line that is drawn in the figure corresponds to the formula

$$P_{\rm min} = 1.31^S \cdot 190 \text{ d}$$

where S stands for the M subtype (e.g. $S = 3$ for spectral type M3).

This limit can be interpreted in terms of binary geometry, because the spectral type is related to the radius R of the giant and the period is related to the binary separation:

- Radii of cool M giants of different spectral subtypes are given by Dumm & Schild (1998). We adopted their respective (median) values.
- The orbital period is related to the binary separation through Kepler's third law. Instead of the binary separation we computed the distance, ℓ_1, from the center of the cool star to the inner Lagrangian point L_1. For this we had to adopt a circular orbit and masses for both stars. We adopted $M_{\rm wd} = 0.6\ M_\odot$ and $M_{\rm rg} = 1.4\ M_\odot$ for the hot and the cool components respectively. These are typical values (see e.g. Schmutz et al. 1994; Schild et al. 1996). An increase in the total mass would have the effect of shifting ℓ_1 to slightly larger values: doubling the total mass, results in an increase of ℓ_1 by $\Delta \log(\ell_1) = 0.1$. Reversing the mass ratio has approximately the same effect, but in the opposite direction.

In Fig. 8 we show ℓ_1 vs. R for the systems of spectral type M. The diagram looks still similar to Fig. 7 (except for the confinement to spectral class M). The three dashed lines indicate the locii $\ell_1 = R$, $\ell_1 = 2 \cdot R$, and $\ell_1 = 4 \cdot R$. The systems clustering at the period limit are now located

close to $\ell_1 = 2 \cdot R$, with only T CrB far below. Hence, the limit evidently corresponds to a configuration where the red giant's photosphere reaches about half way out to L_1: $R \lesssim \frac{1}{2} \cdot \ell_1$.

We therefore believe that the period limit is in fact a restriction to the radius of the red giant. Under these conditions the system should be well detached. If the photosphere of the cool giant further approaches the Lagrangian critical surface the symbiotic phenomenon either disappears or becomes short living. We speculate that dynamical mass exchange would start, leading to an object that is no more regarded as a symbiotic star.

On the other hand, the cool star in T CrB, according to Fig. 8, fills its Roche lobe. This interpretation fits perfectly with its periodic light variations that are attributed to the ellipsoidal shape of the red giant due to the tidal distortions caused by the companion (e.g. Belczyński & Mikołajewska 1998). Strong ellipsoidal light variations are rarely observed for symbiotic stars. T CrB is a peculiar symbiotic, in that it belongs at the same time also to the class of recurrent novae with fast, large amplitude outbursts. It differs also from other symbiotics by the fact that the hot companion is more massive than the cool giant. According to current mass transfer theories, this property prevents dynamically unstable Roche lobe overflow from the cool giant (see Belczyński & Mikołajewska 1998). A similar but much weaker ellipticity effect has also been found in the light curve of EG And (Wilson & Vaccaro 1997). This seems to suggest that $R > \ell_1/2$ for this object (e.g. $R \approx 0.8\ell_1$ when adopting a large inclination as expected for an eclipsing system) in contradiction with Fig. 8. However, as discussed in Wilson & Vaccaro (1997) such a large radius for the red giant is in contradiction with current estimates for the distance of the EG And system. One possible solution of this problem could be, that radiation pressure lowers the effective surface gravity of the red giant, so that the tidal distortions are significantly enhanced and could therefore already be visible for $R \approx \ell/2$ (see e.g. Drechsel et al. 1995).

There exist systems with $\ell_1 \gg 2 \cdot R$, but the symbiotic phenomena are possibly less pronounced unless the wider separation is compensated by another property (e.g. a higher luminosity of the white dwarf). In terms of orbital period, the widest systems lie on the dashed line in Fig. 7. This line corresponds to a period $P_{\max} = 1.20^S \cdot 1660$ d.

There is possibly a tendency for the classical symbiotic variables (Z And type) to cluster closer to the $P_{\min}$ limiting ratio than the symbiotic novae and those objects with less prominent outburst activity.

7. Evolutionary considerations

Elaborate theoretical studies on the formation and evolution of symbiotic systems have been made recently, e.g. by Yungelson et al. (1995), Han et al. (1995) and Iben & Tutukov (1996). These investigations provide a very comprehensive picture of our present understanding of these systems and they reproduce successfully many observed properties. However, they also show that much work still needs to be done in order to fully understand the interaction processes and the complex evolutionary phenomena in symbiotic systems.

We will not repeat the findings of the mentioned works but only address a few topics where our statistical analysis of the spectral types for the red giants in symbiotic systems may help clarifying the current understanding.

7.1. Where are the main-sequence accretors?

It is generally accepted that most symbiotic binaries are detached systems consisting of a red giant and a white dwarf. Accretion at a rate of 10^{-9} to 10^{-7} $M_\odot$/yr is probably due to capture from a wind emitted by the giant. The activity of the hot component is explained as nuclear burning of the accreted hydrogen-rich matter (e.g. Tutukov & Yungelson 1976).

However, for very few systems a physically distinct model is often advocated: a binary system consisting of a Roche-lobe filling red giant and a low-mass main-sequence accretor (see e.g. Kenyon & Webbink 1984; Kenyon 1992). With new observations this class has been shrinking and currently there are only very few systems left, like AX Per and CI Cyg, where comprehensive observational studies support, or at least do not exclude, this possiblity (e.g. Mikołajewska & Kenyon 1996b). We believe that a "normal", detached system with the white dwarf companion cannot be ruled out for AX Per nor CI Cyg. Because both systems are eclipsing the interpretation of the observational data is complicated due to the possible presence of obscuring matter in the orbital plane. In our period–spectral type and $R - \ell_1$-diagrams both, AX Per and CI Cyg, are located near the limiting line, in the midst of the other symbiotic systems. In particular, their location indicates that they are detached systems. Also, AX Per and CI Cyg do not show periodic (double wave per orbital period) photometric variations of $\approx 0\overset{\mathrm{m}}{.}3$ in the V-band as expected for a tidally distorted, Roche-lobe filling red giant.

These findings argue against the main sequence accretor model requiring very high mass transfer rates ($\dot{M} \sim 10^{-5}\, M_\odot$/yr) in order to yield the high luminosity of the ionizing radiation source. Such high transfer rates are only expected for Roche-lobe overflow in a semi-detached system. Thus, we propose that AX Per and CI Cyg could be detached systems with white dwarf companions because they seem to obey the general $\ell_1 = 2 \cdot R$ limit as well.

The controversy on the interpretation of the AX Per and CI Cyg systems also opens the more general question, whether a red giant with a main sequence accretor can indeed produce enough ionizing radiation for producing the

higher excitation emission lines, which are characteristic for symbiotic binaries.

7.2. Distribution of periods

According to the previous sections the distribution of spectral types is strongly biased towards late spectral types. Further, we found the spectral types or the radii of the red giants to be correlated with the orbital periods, indicating that there exists a similar strong bias in the period distribution. In fact, the distribution of periods for symbiotic systems peaks around 2 years. No system is known with $P < 200$ days, and only 2 systems in Table 6 have a period above 4 years.

The short period cut-off for symbiotic systems is comparable to the period cut-off found for barium-star type binaries, indicating a close relationship. The barium-star type systems are composed of a red giant with an abundance anomaly (s-process elements enhanced) and a white dwarf (e.g. McClure & Woodsworth 1990; Jorissen & Mayor 1992). The abundance peculiarity is explained by mass transfer from the companion which has undergone AGB-star evolution and is now a white dwarf. For shorter period double star systems such a phase of heavy mass transfer from a cool giant is probably dynamically unstable and will end up in a short period system ($P \ll 10$ days) similar to catalcysmic binaries (e.g. Paczyński 1976; Meyer & Meyer-Hofmeister 1979; Iben & Tutukov 1984). Thus, the presence of a white dwarf naturally explains the paucity of short orbital periods ($P < 1$ year) for symbiotic and barium-star type binaries. In fact, there are several symbiotic systems known with a barium-star like abundance anomaly (e.g. Smith et al. 1996, 1997). If red giants with main sequence accretors are viable symbiotic binary models then it is not clear why there are no systems with shorter periods around $50 - 200$ days.

Only few symbiotic systems with orbital period beyond 1500 days are known (see Table 4). This is in contrast to the barium-stars which show a period distribution extending well to 3000 days or even beyond (Jorissen 1997). Selection effects for such a comparison are certainly important, particularly when considering that no periods are known for symbiotic miras. Nontheless, the available period distribution for the subsample of s-type symbiotic systems should be quite representative, and this shows a clear deficiency for long period systems when compared to barium stars. Possibly, the mass transfer and, in consequence, symbiotic activity is reduced for very large orbital separations corresponding to periods $P > 1500$ days, even for the quite rare case where the cool star reaches the large radius of a very late M giant of spectral type M6 or M7. Thus the strong peak in the spectral type distribution around $M4 - M5$ for the red giants in symbiotic systems reflects the orbital period distribution with its maximum around 500 to 700 days.

Symbiotic activity for much longer period systems is again possible if the cool giant has a substantially enhanced mass loss. Such strongly enhanced mass loss rates are observed for luminous AGB stars like the mira-variables with dust shells. The corresponding class are the d-type symbiotic systems. Unfortunately, nothing firm is known about their period distribution. The expectation for the orbital periods are very long ($P \gg 20$ years).

8. Discussion and conclusions

Symbiotic binaries are a heterogeneous class of objects. Therefore, the determination of system parameters turns out to be hampered often by some peculiar property of the individual object. This makes a statistical analysis of basic system parameters for symbiotic systems difficult. For example, there are entire subgroups, like the d-type symbiotics, for which we do not even know the orbital period of a single system.

The spectral type of the red giant is certainly a parameter, which is most readily available. But even the determination of this parameter requires a careful assessment of the specialties of symbiotic spectra. So it is in most cases not possible to use the traditional classification criteria in the blue (photographic) spectral region, because there, the emission from the ionized nebula and/or from the hot component often dominates the spectrum. Even the use of the red spectral region may give erroneous results (see Sect. 3) if the veiling by the nebular emission is not taken properly into account.

We based our determination of spectral types on near-IR spectra of molecular bands. In this spectral region the above mentioned problems can often be avoided, because the red giant spectrum is much more prominent and the nebular emission is in most cases negligible. Nonetheless, the diversity of symbiotic systems requires still a special treatment for some objects. For instance, we had to use blue spectra for giants with earlier spectral types having no molecular bands in the near IR. Still, a few of the observed systems escaped classification because the red giant is heavily obscured by dust and no spectral features are visible in the $4000 - 9000$ Å region.

We determined the spectral type of the cool giant in about 100 symbiotic systems. Together with literature data we collected classifications in about 170 systems. This is unique in the sense that no other parameter is known for almost the complete sample of symbiotic systems, including all subgroups.

Our study further supports and elucidates the finding that the red giants in symbiotic systems are strongly biased towards late spectral types. While the frequency of M subtypes in the solar neighbourhood is decreasing from M0 to M8, the distribution of the symbiotic systems peaks at M5. Similarly, the relative frequency of mira variables is 6 times larger in symbiotic systems. For M-giants late spectral types are associated with large stellar radii,

with extended atmospheres, and with heavy mass loss. The predominance of very late M-giants in symbiotic systems indicates that these properties are key ingredients for triggering symbiotic activity.

A major result of this study is the strong correlation between the spectral type of the cool giant and the orbital period. The distribution of objects in the spectral type – orbital period diagram indicates that there exists for a given spectral type a lower limit for the orbital period, which is about 250 d for spectral type M1, 560 d for M4, and 1260 d for M7. Only one system, the recurrent novae T CrB, lies clearly below this limit, suggesting that its very individual properties may be related to this exceptional feature.

Very interesting conclusions emerge when the spectral types and the orbital periods are converted into photospheric radii and critical Roche lobe radii, respectively. We find that the limiting line from the spectral type – orbital period diagram is practically identical with the relation $\ell_1 = 2 \cdot R$, where ℓ_1 is the distance from the center of the cool giant to the Lagrangian point L_1, and R is the red giant's radius. This strongly suggests that at least most symbiotic systems are well detached. A large fraction of the systems cluster close to the $\ell_1 = 2 \cdot R$ limit, suggesting that this configuration is ideal for producing strong and long-lived symbiotic activity on the companion.

The present catalogue of spectral types for the cool giants in symbiotic systems may provide an important input for further statistical studies. Spectroscopic parallaxes based on the spectral types could provide a better assessment of the space frequency and the galactic distribution of symbiotic systems. In particular a comparison with related objects, like barium star type binaries or planetary nebulae with double star nuclei could clarify the evolutionary status and the interaction processes of symbiotic systems.

Acknowledgements. It is a pleasure to thank Regina E. Schulte-Ladbeck for allowing us to use her spectral data. We thank our colleagues Thomas Dumm, Orsola De Marco, Joachim Krautter, Harry Nussbaumer, Hans Schild, and Werner Schmutz for many useful comments. HMS acknowledges financial support by the Deutsche Forschungsgemeinschaft (KR 1053/6-1).

References

Aaronson M., Liebert J., Stocke J., 1982, ApJ 254, 507
Allen D.A., 1978, IBVS 1399
Allen D.A., 1980, MNRAS 192, 521
Allen D.A., 1982, in The Nature of Symbiotic Stars, IAU Coll. No. 70, Friedjung M., Viotti R. (eds.). Reidel, p. 27
Allen D.A., 1984, Proc. Astron. Soc. Aust. 5, 369
Arkhipova V.P., Ikonnikova N.P., Noskova R.I., 1995, Astron. Lett. 21, 339
Belczyński K., Mikołajewska J., 1998, MNRAS 296, 77
Belyakina T.S., Prokof'eva V.V., 1991, SvA 35, 154
Bruch A., Niehues M., Jones A.F., 1994, A&A 287, 829
Cieslinski D., Elizalde R., Steiner J.E., 1994, A&AS 106, 243
Cieslinski D., Steiner J.E., Elizalde F., Pereira M.G., 1997, A&AS 124, 57
Cieslinski D., Steiner J.E., Jablonski F.J., 1998, A&AS 131, 219
Davidsen A., Malina R., Bowyer S., 1977, ApJ 211, 866
Dobrzycka D., Kenyon S.J., 1994, AJ 108, 2259
Dobrzycka D., Kenyon S.J., Mikołajewska J., 1993, AJ 106, 284
Downes R.A., Keyes C.D., 1988, AJ 96, 777
Drechsel H., Haas S., Lorenz R., Gayler S., 1995, A&A 294, 723
Dumm T., Schild H., 1998, New Astron. 3, 137
Dumm T., Mürset U., Nussbaumer H., Schild H., Schmid H.M., Schmutz W., Shore S.N., 1998, A&A 336, 637
Duerbeck H.W., Seitter W.C., 1989, PASP 101, 673
Dyck H.M., Benson J.A., Van Belle G.T., Ridgway S.T., 1996, AJ 111, 1705
ESA, 1997, The Hipparcos Catalogue, ESA SP-1200
Fernie J.D., 1985, PASP 97, 653
Han Z., Eggleton P.P., Podsiadlowski P., Tout C.A., 1995, MNRAS 277, 1443
Harries T.J., Howarth I.D., 1996, A&AS 119, 61
Hinkle K.H., Fekel F.C., Johnson D.S., Scharlach W.W.G., 1993, AJ 105, 1074
Hoffleit D., 1968, Irish Astron. J. 8, 149
Hoffleit D., 1970, Inf. Bull. Var. Stars 469
Iben, I.Jr., Tutukov A.V., 1984, ApJS 54, 335
Iben, I.Jr., Tutukov A.V., 1996, ApJS 105, 145
Jaschek C., Jaschek M., 1987, The classification of stars. Cambridge
Jorissen A., 1997, in: Physical Processes in Symbiotic Binaries and Related Systems, Mikołajewska J. (ed.). Copernicus Found. for Polish Astron., Warsaw, p. 135
Jorissen A., Mayor M., 1992, A&A 260, 115
Keenan P.C., Hynek J.A., 1945, ApJ 101, 265
Keenan P.C., McNeil R.C., 1976, An atlas of spectra of the cooler stars, Ohio State Univ. Press
Keenan P.C., McNeil R.C., 1989, ApJS 71, 245
Keenan P.C., Morgan W.W., 1941, ApJ 94, 501
Kenyon S.J., 1986, The symbiotic stars. Cambridge University Press
Kenyon S.J., 1992, in: Evolutionary Processes in Interacting Binary Stars, IAU Symp. 151, Kondo Y. et al. (eds.), p. 137
Kenyon S.J., Fernández-Castro T., 1987, AJ 93, 938
Kenyon S.J., Garcia M.R., 1986, AJ 91, 125
Kenyon S.J., Mikołajewska J., 1995, AJ 110, 391
Kenyon S.J., Webbink R.F., 1984, ApJ 279, 252
Kenyon S.J., Mikołajewska J., Mikołajewski M., Polidan R.S., Slovak M.H., 1993, AJ 106, 1573
Kenyon S.J., Oliversen N.A., Mikołajewska J., Mikołajewski M., Stencel R.E., Garcia M.R., Anderson C.M., 1991, AJ 101, 637
Kolotilov E.A., Munari U., Yudin B.F., 1995a, A&A 293, 815
Kolotilov E.A., Munari U., Yudin B.F., 1995b, MNRAS 275, 185
Mayall M.W., 1937, Harvard Ann. 105, 491
McClure R.D., Woodsworth A.W., 1990, ApJ 352, 709
Medina Tanco G.A., Steiner J.E., 1995, AJ 109, 1770
Meinunger L., 1979, IBVS 1611

Meyer F., Meyer-Hofmeister H., 1979, A&A 78, 167
Michalitsianos A.G., Maran S.P., Oliversen R.J., Bopp B., Kontizas E., Dapergolas A., Kontizas M., 1991, ApJ 371, 761
Mikołajewska J., 1997, in: Physical Processes in Symbiotic Binaries and Related Systems, Mikołajewska J. (ed.). Copernicus Found. for Polish Astron., Warsaw, p. 3
Mikołajewska J., Kenyon S.J., 1992a, AJ 103, 579
Mikołajewska J., Kenyon S.J., 1992b, MNRAS 256, 177
Mikołajewska J., Kenyon S.J., 1996, AJ 112, 1659
Mikołajewska J., Kenyon S.J., Mikołajewski M., 1989, AJ 98, 1427
Mikołajewska J., Acker A., Stenholm B., 1997, A&A 327, 191
Morgan D.H., 1996, MNRAS 279, 301
Munari U., 1992, A&A 257, 163
Munari U., 1993, A&A 273, 425
Munari U., Marconi R., Stagni R., 1990, MNRAS 242, 653
Munari U., Whitelock P.A., Gilmore A.C., Blanco C., Massone G., Schmeer P., 1992, AJ 104, 262
Munari U., Yudin B.F., Kolotilov E.A., Gilmore A.C., 1995, AJ 109, 1740
Mürset U., Schild H., Vogel M., 1996, A&A 307, 516
Osterbrock D.E., 1989, Astrophys. of Gaseous Nebulae and Active Galactic Nuclei. Univ. Science Books, Mill Valley, California
Paczyński B., 1976, IAU Symp. 73, 75
Pavlenko E.P., Bochkov V.V., Vasil'yanovskaya O.P., 1996, Astrophys. 39, 15 (Astrofizika 39, 31)
Pereira C.B., Vogel M., Nussbaumer H., 1995, A&A 293, 783
Pucinskas A., 1970, Bull. Vil. Univ. Astron. Obs. 27, 24
Ramsey L.W., 1981, AJ 86, 557
Reimers D., 1975, in: Problems in Stellar Atmospheres and Envelopes, Baschek B. et al. (eds). Springer, Berlin, p. 229
Rejkuba M., Munari U., Hazen M., Mattei J., Schweitzer E., Shugarov S., Yudin B., 1997, in: Physical Processes in Symbiotic Binaries and Related Systems, Mikołajewska J. (ed.). Copernicus Found. for Polish Astron., Warsaw, p. 193
Schild H., Schmid H.M., 1997, A&A 324, 606
Schild H., Boyle S.J., Schmid H.M., 1992, MNRAS 258, 95
Schild H., Mürset U., Schmutz W., 1996, A&A 306, 477
Schmid H.M., 1994, A&A 284, 156
Schmid H.M., Nussbaumer H., 1993, A&A 268, 159
Schmid H.M., Schild H., 1994, A&A 281, 145
Schmid H.M., Dumm T., Mürset U., Nussbaumer H., Schild H., Schmutz W., 1998, A&A 329, 986
Schmutz W., Schild H., Mürset U., Schmid H.M., 1994, A&A 288, 819
Schulte-Ladbeck R.E., 1988, A&A 189, 97
Sharpless S., 1956, ApJ 124, 342
Smith V.V., Cunha K., Jorissen A., Boffin H.M.J., 1996, A&A 315, 179
Smith V.V., Cunha K., Jorissen A., Boffin H.M.J., 1997, A&A 324, 97
Swope H.H., 1941, ApJ 94, 140
Tutukov A.V., Yungelson L.R., 1976, Astrophysics 12, 342
van Leeuwen F., Feast M.W., Whitelock P.A., Yudin B., 1997, MNRAS 287, 955
Van Winckel H., Schwarz H.E., Duerbeck H.W., Fuhrmann B., 1994, A&A 285, 241
Webster B.L., Allen D.A., 1975, MNRAS 171, 171
Whitelock P.A., 1987, PASP 99, 573
Wilson R.E., Vaccaro T.R., 1997, MNRAS 291, 54
Yamashita Y., 1972, Ann. Tokyo Astron. Obs. 13, 169
Yamashita Y., Nariai K, Norimoto Y., 1977, An Atlas of Representative Stellar Spectra. Univ. of Tokyo Press
Yungelson L., Livio M., Tutukov A., Kenyon S.J., 1995, ApJ 447, 656